Defect Scars on Flexible Surfaces with Crystalline Order

Tamotsu Kohyama[1,2] and Gerhard Gompper[1,*]

[1]*Institut für Festkörperforschung, Forschungszentrum Jülich, 52425 Jülich, Germany*
[2]*Faculty of Education, Shiga University, Hiratsu 2-5-1, Otsu, Shiga, 520-0862, Japan*

(Received 13 January 2007; published 7 May 2007)

The crystallography of two-dimensional particle packings on flexible surfaces of spherical topology is investigated. Examples are viral capsids and crystalline vesicles. Computer simulations of dynamically triangulated surfaces are employed to study the shape and structure of lattice defects as a function of the Föppl–von Kármán number γ. We find that grain-boundary scars become much more fuzzy with increasing temperature, that the size of grain-boundary scars saturates with increasing vesicle radius, and that the buckling transition shifts to higher values of γ due to the presence of scars.

DOI: 10.1103/PhysRevLett.98.198101 PACS numbers: 87.16.Dg, 81.16.Dn, 61.72.Bb

Self-assembled crystalline membrane structures have been observed in systems as diverse as mixtures of anionic and cationic surfactants forming vesicles [1], proteins in viral capsids [2–6], and clathrin-coated pits at the plasma membrane of cells [7,8]. However, long-range crystalline order and nonzero Gaussian curvature are incompatible. A perfect two-dimensional crystal thus cannot exist, for example, on the surface of a sphere. The question is then how the crystal adapts to a curved space. For two-dimensional crystals with preferred sixfold coordination on a surface of spherical topology, Euler's formula indicates that there must be topological lattice defects; in the simplest case 12 fivefold disclinations. However, this does not have to be the defect configuration of minimal stretching energy. Instead, dislocations (pairs of five- and sevenfold disclinations) can be generated to screen the long-range strain field around the 12 topological disclinations. Indeed, it was shown recently [9–12] that the lowest-energy state of a crystal on a sphere is a configuration, in which each topological fivefold disclination is accompanied by a line of dislocations, a grain boundary of *finite* length, which scales *linearly* with the sphere radius [11,12]. These "defect scars" have already been observed in colloidal crystals on the surface of spherical emulsion droplets [13–15].

However, in many cases, a crystal is *not* forced to be on the surface of a sphere, but can adjust its shape, for example, in viral capsids [2,4,6] and surfactant vesicles [1]. Therefore, we investigate in this letter the defect patterns, which form due to the competition of curvature elasticity and crystalline order on *flexible* vesicles of spherical topology. Furthermore, we take into account thermal fluctuations. Spherical vesicle shapes are recovered in the limit of large bending rigidity κ. In the opposite limit, where the dimensionless Föppl–von Kármán number $\gamma = K_0R^2/\kappa$—with the two-dimensional Young modulus K_0 and vesicle radius R—is large, it has been shown that a lattice with exactly 12 fivefold disclinations approaches an icosahedral shape, in which bending and stretching energy is localized in "stretching ridges" connecting the disclinations [16]. What happens to the grain-boundary scars in the large-γ limit? What is the effect of thermal fluctuations on the size and shape of grain-boundary scars? We show by computer simulations of crystalline membranes that for any given elastic parameters, the scar length saturates with increasing vesicle radius. Furthermore, while the scar shape at finite temperature T deviates strongly from the linear $T = 0$ shape, its size remains essentially unaffected.

We employ a dynamically triangulated surface model of flexible membranes [17,18]. The vesicle is modeled by a triangular network of spherical topology, with a curvature energy E_b given by the discretized Laplacian [17]. Bonds connecting neighboring vertices represent a tethering potential, which prevents bonds from exceeding the maximum tether length ℓ_0 and vanishes otherwise. In addition, all vertices have hard-sphere interactions with sphere diameter σ_0. Monte Carlo simulations of this model consist of vertex moves and bond-flips between two adjacent triangles. For flat membranes, a crystalline phase exists for small bond lengths ℓ_0 [19]. In this phase, bond flips allow the formation, migration, and annihilation of crystal defects in thermal equilibrium. After equilibration, averages are typically calculated over 10 to 100×10^6 Monte Carlo steps (MCS) per vertex.

The Young modulus K_0 is a monotonically decreasing function of the tether length ℓ_0. All results presented here were obtained for tether length $\ell_0/\sigma_0 = 1.45$, for which the two-dimensional Young modulus has been estimated in Ref. [20] to be $K_0a^2/k_BT \simeq 78$, where $a \simeq (\sigma_0 + \ell_0)/2$ is the average bond length. This value of the Young modulus indicates that our system is not close, but also not too far from the transition to the hexatic phase of a *flat* membrane, which occurs at $K_0a^2/k_BT = 16\pi = 50.26$ [21] corresponding to a tether length of $\ell_0/\sigma_0 \simeq 1.480$ [19]. In thermally undulating membranes of sufficiently large size, the crystalline phase is unstable and is replaced by the hexatic phase [22,23].

Two typical configurations of vesicles of different size are shown in Fig. 1. This demonstrates the three main results of our simulations, which we will discuss in more detail below: (i) grain-boundary scars exist for all vesicle radii R, but are much more fuzzy than at $T = 0$, (ii) vesicles

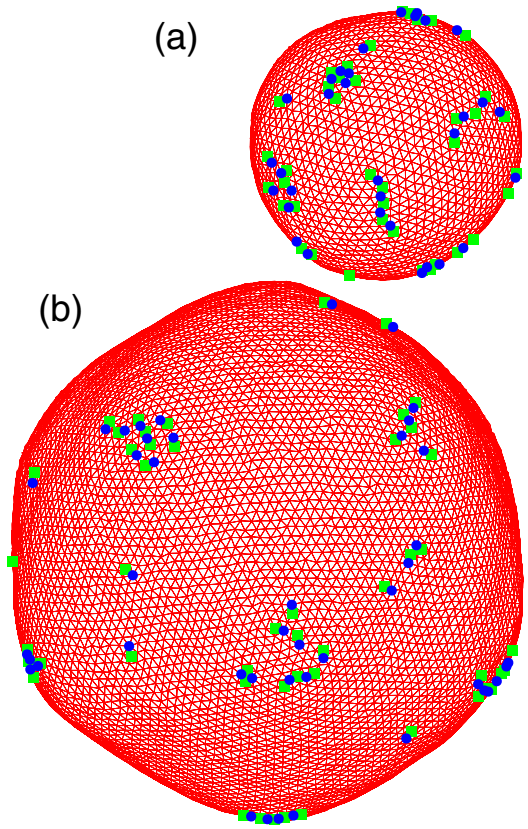

FIG. 1 (color online). Snapshots of vesicle shapes and defect configurations for bending rigidity $\kappa/k_BT = 100$ and system size N, with (a) $N = 2562$ (after 109×10^6 MCS), and (b) $N = 10\,242$ (after 18×10^6 MCS). Five- and sevenfold coordinated vertices are shown by (green) squares and (blue) dots, respectively.

become more faceted with increasing R, as they do in the absence of lattice defects, and (iii) the size of grain-boundary scars relative to the vesicle radius decreases with increasing R.

The dependence of the average size of grain-boundary scars as a function of the vesicle radius is shown in Fig. 2 for three bending rigidities. Since the scars are not simply lines of neighboring disclinations, we define the scar size globally as the number $L = \langle N_5 + N_7 - 12\rangle/24$, where N_5 and N_7 are the total number of five- and sevenfold disclinations, respectively. Thus, L is the average number of excess dislocations in each scar. Figure 2 shows that for very small radii $R/a < 2.5$, the number of dislocations is extremely small. For $R/a > 2.5$, but when the vesicle shape is still essentially spherical, the scar size is found to increase *linearly* with R. The slope of this line agrees very well with the theoretical prediction [11] of $(\pi/3) \times [\sqrt{11} - 5\cos^{-1}(5/6)](R/a) \simeq 0.41(R/a)$ for $T = 0$, as well as with experimental observations for colloidal crystals at the surface of (spherical) emulsion droplets [13]. For larger radii, the scar length saturates. The critical radius R_c where this happens, increases with increasing bending rigidity.

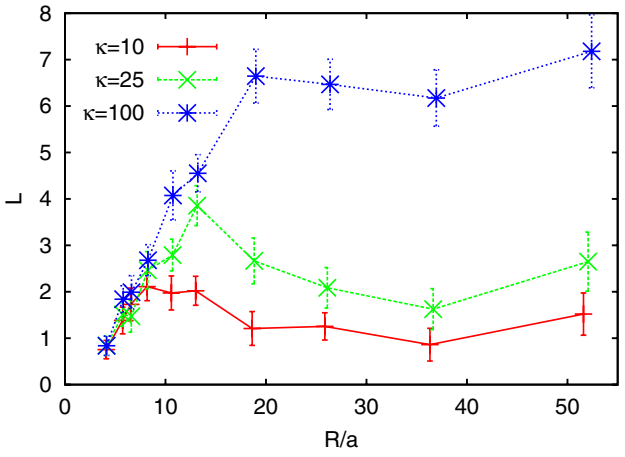

FIG. 2 (color online). Scar size L, defined by the average number of excess dislocations per topological disclination, as a function of the vesicle radius for various bending rigidities, as indicated.

A better understanding of the different regimes and the crossover between them can be obtained by considering the bending and stretching contributions in the elastic energy. For small Föppl–von Kármán numbers $\gamma = K_0R^2/\kappa$, the vesicles are spherical and can reduce their energy by grain-boundary scars [11]. For vesicles *without defects* (except for the 12 "topological" disclinations), the icosahedral shape begins to emerge for $\gamma > \gamma_b \simeq 150$. In the regime $150 < \gamma < 10^4$, the elastic energy can be approximated very well by assuming a superposition of 12 cylindrical cones with a flat inner region near the tip [2]. The size of the flat region is determined by the buckling radius $R_b \simeq (150\kappa/K_0)^{1/2}$. We can modify this estimate slightly by assuming that the inner region is not flat, but a spherical cap with a radius of curvature proportional to R_b—consistent with the vesicle shapes obtained from energy minimization in Ref. [2]. This does not change the functional dependence of the inner region, which still scales as $K_0R_b^2$ [11]. If the vesicle shape is not strongly affected by the scars, then this picture implies that the scars grow linearly with the vesicle radius for $\gamma < \gamma_b$, but are then restricted to the spherical-cap regions near the corners of the icosahedron, since in the faceted regions of nearly *vanishing* Gaussian curvature the energy cannot be reduced by the presence of scars. Thus, the scar size for $R > R_b$ should be approximately the same as for $R = R_b$.

This argument implies that the scaled scar size $L/(R/a - 2.5)$ should be a universal function of R/R_b, where R is the average vesicle radius, or equivalently of γ. Indeed, we find that the curves for the three values of the bending rigidity in Fig. 2 all collapse onto a single master curve when plotted in this way; see Fig. 3. For R larger than the buckling radius, the scar length saturates, which implies that $L/(R/a - 2.5)$ decays as R^{-1} or $\gamma^{-1/2}$. The crossover between the two regimes occurs at $\gamma \simeq 350$, which is about twice as large as γ_b. The reason is that the simple scaling picture developed above ignores two

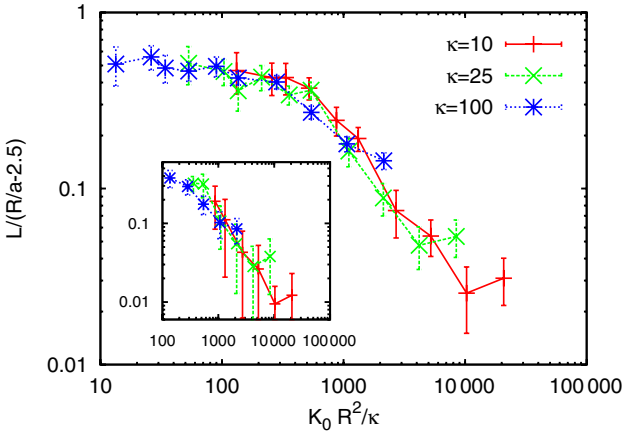

FIG. 3 (color online). Scaled scar size, $L/(R/a-2.5)$, as a function of the Föppl–von Kármán number $\gamma = K_0R^2/\kappa$, for various bending rigidities as indicated. The inset shows the scaled average size, $\langle n_{\text{odd}}\rangle/(R/a-2.5)$, of defect clusters with an odd number of defects as a function of γ.

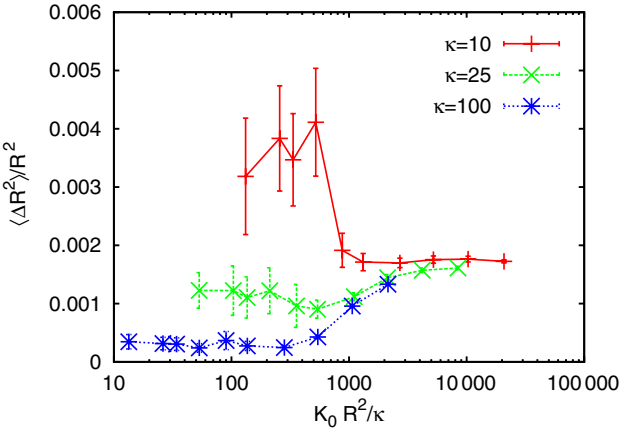

FIG. 4 (color online). Mean squared asphericity, $A = \langle\Delta R^2\rangle/\langle R\rangle^2$, as a function of the Föppl–von Kármán number γ, for various bending rigidities κ as indicated.

effects: (i) the change of the energy of the spherical caps due to the presence of the scars, and (ii) the thermal fluctuations of the vesicle shape. The effect of the scars can be calculated, following Ref. [2], by considering the vesicle as being composed of 12 buckled disclinations with a spherical tip. This implies the elastic energy

$$E = 4\pi\kappa \ln(R/R_b) + c_n \frac{\pi}{36} K_0 R_b^2, \tag{1}$$

where c_n is a constant for scars containing n dislocations, which has been calculated in Ref. [11]. By minimizing Eq. (1) with respect to R_b, we find

$$\gamma_b(n) \equiv \frac{K_0 R_b(n)^2}{\kappa} = \frac{72}{c_n}. \tag{2}$$

With $c_0 = 0.60$, $c_1 = 0.44$, $c_2 = 0.37$, and $c_4 = 0.32$ [11], Eq. (2) indicates that for scars of moderate length, the buckling threshold increases to a value about twice as large as for vesicles without scars. This explains the behavior observed in the simulations for large κ. For $\kappa/k_BT = 10$, we believe that thermal shape fluctuations play an important role. In this case, out-of-plane membrane fluctuations and grain-boundary scars compete to screen the long-range strain field of fivefold disclinations.

Figure 4 shows the mean squared asphericity, $A \equiv \langle\Delta R^2\rangle/\langle R\rangle^2 = \frac{1}{N}\sum_i \langle(R_i - \langle R\rangle)^2\rangle/\langle R\rangle^2$, as a function of the Föppl–von Kármán number. The three curves for different κ converge to the same value $A \simeq 0.0017$ after the shape transition from spherical to icosahedral shell, where the transition occurs around $\gamma^* \simeq 1000$. This value of A is in reasonable agreement with the value $A_{\text{ico}} = 0.0021$ of a perfect icosahedron. For $\gamma < \gamma^*$, the vesicles should behave essentially like spherical fluid membranes, so that the amplitude of the fluctuation can be estimated to be $\langle\Delta R^2\rangle/\langle R\rangle^2 = (k_BT/\kappa)\sum_{l\geq 2}(2l+1)/[4\pi l(l-1)\times(l+1)(l+2)] = k_BT/(12\pi\kappa)$, in good agreement with the numerical results of Fig. 4. Thus, for small bending rigidities, increasing vesicle size strongly *reduces* the asphericity due to a reduction of thermal fluctuations.

In order to investigate the structure and fluctuations of defect scars in more detail, we now define defect clusters as all disclination sites, which have a maximum distance of three lattice constants between neighboring defects. The size n of a cluster is its number of defect sites. The results are shown in Fig. 5 for clusters of odd and even sizes—where odd sizes correspond to scars, with *one* topological disclination and several dislocations. This allows several conclusions. First, the distribution of clusters of odd sizes has a broad peak for $\kappa/k_BT = 100$ (and sufficiently large N so that scars are well developed). The fluctuations of the cluster size are very pronounced, since the width of the distribution is approximately equal to the peak position. On the other hand, only very small clusters of even sizes appear, which correspond to single dislocations and bound

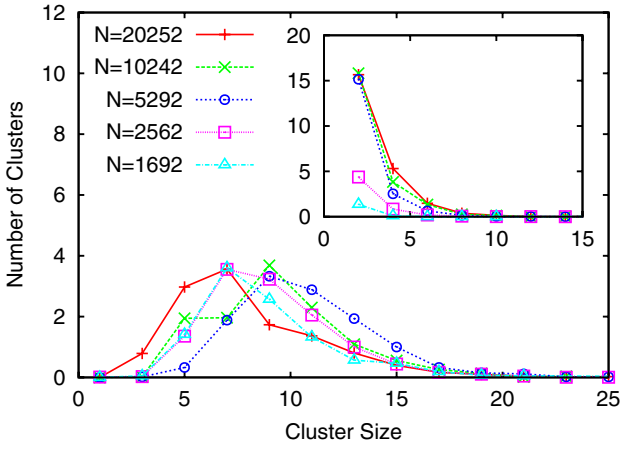

FIG. 5 (color online). Distribution of scars sizes with an odd number of defects for $\kappa/k_BT = 100$, and various system sizes as indicated. The insets show the distributions of defect clusters with an even number of defects.

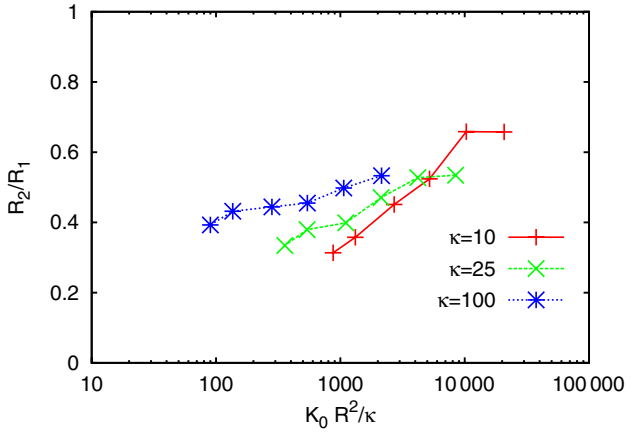

FIG. 6 (color online). Sphericity R_2/R_1 (see text) of scars with more than three defects as a function of the sphere radius, for $\kappa/k_BT = 10$, $\kappa/k_BT = 25$, and $\kappa/k_BT = 100$.

dislocations pairs. Second, the average size of "odd" clusters, a measure of the scar length, is shown as an inset in Fig. 3; it follows essentially the same scaling function as the number L of excess dislocations. This demonstrates that "isolated" dislocations play a minor role, since they are taken into account in L, but not in the defect clusters. Third, the number of clusters of size $n = 4$ increases with increasing vesicle radius for all investigated κ-values. This happens because dislocation pairs are excited thermally, so that their number should increase proportional to the membrane area.

Scars are not straight defect lines at finite temperatures, as can be seen very clearly in the configurations of Fig. 1. We therefore characterize their shape by the eigenvalues R_1^2 and R_2^2, with $R_1 \geq R_2$, of the gyration tensor $G_{\alpha\beta} = \sum_i r_\alpha^{(i)} r_\beta^{(i)}$, where $\mathbf{r}^{(i)}$ is the position of disclination i in the scar. The results shown in Fig. 6 indicate that the scars (i) have large thermal fluctuations, and thus R_2/R_1 does not show a simple scaling law as a function of γ, and (ii) become less elongated with increasing vesicle radius R.

In comparison, the experiments for colloidal crystals on emulsion droplets in Ref. [14] were performed at a Young modulus of $K_0a^2/k_BT = 167$, i.e., much further away from the crystalline-to-hexatic transition. Therefore, scars are less fuzzy and more elongated.

Viral capsids self-assemble from protein subunits [3], and therefore have the possibility to form scars. We predict that this requires $R/a > 2.5$ (i.e., $N \geq 90$), and $R_b/a \geq 1$ (i.e., $K_0a^2/\kappa \leq 150$). Thus, the icosahedral viruses HK97, yeast L-A [2] and Cowpea chlorotic mottle virus (CCMV) [24] (for which elastic coefficients have been determined) are all too small in size to show scars. With $K_0/\kappa \simeq 1.5\ \mathrm{nm}^{-2}$ [2] and $a \simeq 10$ nm, their elasticity is at the borderline of scar formation. If all viruses have similar elastic coefficients, as speculated in Ref. [2], this would explain why scars have not been observed on viruses so far.

Stimulating discussions with A. R. Bausch (TU München), D. M. Kroll (NDSU), and D. R. Nelson (Harvard) are gratefully acknowledged.

*Electronic address: g.gompper@fz-juelich.de

[1] M. Dubois, B. Demé, T. Gulik-Krzywicki, J.-C. Dedieu, C. Vautrin, S. Désert, E. Perez, and T. Zemb, Nature (London) **411**, 672 (2001).
[2] J. Lidmar, L. Mirny, and D. R. Nelson, Phys. Rev. E **68**, 051910 (2003).
[3] R. Zandi, D. Reguera, R. F. Bruinsma, W. M. Gelbart, and J. Rudnick, Proc. Natl. Acad. Sci. U.S.A. **101**, 15 556 (2004).
[4] URL http://viperdb.scripps.edu/.
[5] C. M. Shepherd, I. A. Borelli, G. Lander, P. Natarajan, V. Siddavanahalli, C. Bajaj, J. E. Johnson, C. L. Brooks III, and V. S. Reddy, Nucleic Acids Res. **34**, D386 (2006).
[6] T. T. Nguyen, R. F. Bruinsma, and W. M. Gelbart, Phys. Rev. Lett. **96**, 078102 (2006).
[7] J. Heuser, J. Cell Biol. **108**, 401 (1989).
[8] T. Kohyama, D. M. Kroll, and G. Gompper, Phys. Rev. E **68**, 061905 (2003).
[9] A. Perez-Garrido, M. J. W. Dodgson, and M. A. Moore, Phys. Rev. B **56**, 3640 (1997).
[10] A. Perez-Garrido and M. A. Moore, Phys. Rev. B **60**, 15628 (1999).
[11] M. J. Bowick, D. R. Nelson, and A. Travesset, Phys. Rev. B **62**, 8738 (2000).
[12] M. Bowick, A. Cacciuto, D. R. Nelson, and A. Travesset, Phys. Rev. Lett. **89**, 185502 (2002).
[13] A. Bausch, M. J. Bowick, A. Cacciuto, A. D. Dinsmore, M. F. Hsu, D. R. Nelson, M. G. Nikolaides, A. Travesset, and D. A. Weitz, Science **299**, 1716 (2003).
[14] P. Lipowsky, M. J. Bowick, J. H. Meinke, D. R. Nelson, and A. R. Bausch, Nat. Mater. **4**, 407 (2005).
[15] T. Einert, P. Lipowsky, J. Schilling, M. J. Bowick, and A. R. Bausch, Langmuir **21**, 12 076 (2005).
[16] A. Lobkovsky, S. Gentges, H. Li, D. Morse, and T. A. Witten, Science **270**, 1482 (1995).
[17] G. Gompper and D. M. Kroll, J. Phys. Condens. Matter **9**, 8795 (1997).
[18] G. Gompper and D. M. Kroll, in *Statistical Mechanics of Membranes and Surfaces*, edited by D. R. Nelson, T. Piran, and S. Weinberg (World Scientific, Singapore, 2004), 2nd ed., p. 359.
[19] G. Gompper and D. M. Kroll, Eur. Phys. J. E **1**, 153 (2000).
[20] G. Gompper and D. M. Kroll, J. Phys. I (France) **7**, 1369 (1997).
[21] D. R. Nelson and B. I. Halperin, Phys. Rev. B **19**, 2457 (1979).
[22] H. S. Seung and D. R. Nelson, Phys. Rev. A **38**, 1005 (1988).
[23] G. Gompper and D. M. Kroll, Europhys. Lett. **58**, 60 (2002).
[24] J. P. Michel, I. L. Ivanovska, M. M. Gibbons, W. S. Klug, C. M. Knobler, G. J. L. Wuite, and C. F. Schmidt, Proc. Natl. Acad. Sci. U.S.A. **103**, 6184 (2006).